

edge dislocations normal to the film.

The diffraction pattern from the polymer in the crystalline phase indicates that in this case the polymer chain is fully extended and that a fiber-type order is achieved in a direction perpendicular to this; i.e., there is order between the planes, giving rise the small-angle maxima. The high-resolution images indicate that these planes are relatively straight in the undisturbed regions but can accommodate an extra plane, giving on edge dislocation perpendicular to the film; this leads to considerable distortion of the atomic planes. Only edge dislocations of the 1:0 type were observed.

Therefore, although the electron diffraction patterns would indicate considerable differences between the two structures, the high-resolution micrographs show that there are surprising similarities in one well-defined direction. It also appears that details of molecular geometry are crucial in determining the structure and thus the phase which develops.

With regard to this investigation, the problems regarding the production and physical interpretation of phase contrast and the experimental conditions which are required to orientate the films and image smectic planes have been successfully solved. However, a major problem is still the low signal/noise ratio in the electron micrographs. This becomes particularly important when trying to discover the exact nature of the dislocation core and in deciding to what extent there is some orientation in the spaces between highly ordered regions after short annealing times. In a following paper, we describe approaches to this

problem and the degree of success which has been achieved so far.

Acknowledgment. We are much indebted to Professor Sir Charles Frank for his very helpful and detailed comments on the original manuscript and to Professor H. Ringsdorf for giving us access to the beautiful samples synthesized in his department. We also acknowledge the admirable work of our photographer, E. R. Berger.

Registry No. Poly[oxy[2-[6-[4-(4-cyanophenyl)azo]phenoxy]hexyl]-1,3-dioxo-1,3-propanediyl]oxy-1,6-hexanediyl-1,4-phenyleneazo-1,4-phenyleneoxy-1,6-hexanediyl], 97088-50-1; poly[oxy[1,3-dioxo-2-(2-propenyl)-1,3-propanediyl]oxy-1,6-hexanediyl-1,4-phenyleneazo-1,4-phenyleneoxy-1,6-hexanediyl], 105035-53-8.

References and Notes

- (1) Reck, B.; Ringsdorf, H. *Makromol. Chem., Rapid Commun.* **1985**, *6*, 291.
- (2) Voigt-Martin, I. G.; Durst, H. *Liq. Cryst.* **1987**, *2*, 585.
- (3) Voigt-Martin, I. G.; Durst, H.; Reck, B.; Ringsdorf, H. *Macromolecules* **1988**, *21*, 1620.
- (4) Erickson, H. P.; Klug, A. *Philos. Trans. R. Soc. London, B* **1971**, *B261*, 105.
- (5) Voigt-Martin, I. G.; Durst, H. *Liq. Cryst.* **1987**, *2*, 601.
- (6) Gane, P. A.; Leadbetter, A. J. *J. Phys. C* **1983**, *16*, 2059.
- (7) Richardson, R. M.; Leadbetter, A. J.; Hayter, J. B.; Stirling, W. G.; Gray, G. W.; Tajbakhsh, A. *J. Phys. (Res Ulis, Fr.)* **1984**, *45*, 1061.
- (8) Chandrasekhar, S.; Ranganath, G. S. *Adv. Phys.* **1986**, *35*, 507.
- (9) Zentel, R.; Schmidt, G. F.; Meyer, J.; Benalia, M. *Liq. Cryst.* **1987**, *2*, 651.
- (10) Voigt-Martin, I. G.; Durst, H.; Krug, H., submitted for publication in *Macromolecules*.

X-ray Photoelectron Spectroscopic and Theoretical Study of the Conformational Dependence of the Valence Electronic Levels in Hexagonal and Orthorhombic Poly(oxymethylenes)

P. Boulanger, J. Riga, J. J. Verbist,^{*,†} and J. Delhalle[†]

Laboratoire de Spectroscopie Electronique and Laboratoire de Chimie Théorique Appliquée, Facultés Universitaires Notre-Dame de la Paix, 61, rue de Bruxelles, B-5000 Namur, Belgium. Received September 28, 1987; Revised Manuscript Received February 15, 1988

ABSTRACT: X-ray photoelectron spectroscopy (XPS) valence band spectra of hexagonal and orthorhombic poly(oxymethylenes) are reported and compared with simulated XPS spectra based on ab initio calculations for simple model oligomers $\text{CH}_3\text{O}-(\text{CH}_2\text{O})_x-\text{CH}_3$ where $x = 1, 3, 5$, or 7 . An attempt is made to interpret the observed differences as having a conformational origin.

Introduction

Because of its appropriate sampling depth compared to more classical spectroscopies, XPS (X-ray photoelectron spectroscopy) has been increasingly applied since 1972 to study fundamental structural questions and problems which arise at the surfaces and interfaces of technologically useful polymers. Interest was first focused on the core energy levels, which provide information on the chemical composition, bonding, and (in)homogeneity of the topmost atomic or molecular layers. However, a number of important problems have to do with the discrimination of possible differences between bulk and surface structural

characteristics, the dependence of the latter on the bulk morphologies and preparation, etc.

To implement the description of the situation occurring at polymer surfaces and interfaces, it would be useful to obtain from the same XPS measurements some information about the molecular structure. Unfortunately, this is difficult to obtain from the core levels, which otherwise have the best resolution relative to the other parts of the spectrum.

As demonstrated in 1974 by quantum mechanical simulations and XPS spectra of model polymers,¹ the valence spectral data contain information on the primary and secondary structures of the polymer backbone. A few comparisons^{2,3} between theoretically simulated and measured valence band spectra of pure hydrocarbon polymers have provided a basis for establishing relationships be-

[†] Laboratoire de Spectroscopie Electronique.

^{*} Laboratoire de Chimie Théorique Appliquée.

tween XPS valence band features and the polymer geometrical structure. Such comparisons also confirmed the usefulness of quantum mechanical calculations as an interpretative and predictive tool for polymer XPS valence band spectroscopic measurements. The main limitation comes from the lower photoionization cross sections and from the complexity of this spectral region compared to the well-separated core peaks. This was recently demonstrated in an attempt to search for possible fold signatures in the valence XPS spectra of ordered polyethylene surfaces, showing that there is little hope of relating valence XPS spectral features to naturally occurring conformational structures in saturated hydrocarbons.⁴ Since real polymers may possess complex chemical structures and ill-defined chain geometries, the interpretation of XPS valence bands of polymers which result from a number of bands, possibly overlapping and broadened by various solid-state effects, can be quite difficult. Therefore, we first require carefully assessed signatures for similar effects in relatively simple and well-characterized reference compounds, before it will be reasonable to establish systematic relationships between the XPS valence electronic structure and the surface architecture of more complex polymers.

From theoretical simulations of the valence XPS spectra of three conformations of poly(oxyethylene) (POM), modeled by oligomers corresponding to the formula $\text{CH}_3\text{O}-(\text{CH}_2\text{O})_x-\text{CH}_3$, $x = 1, 3, 5$, and 7 , we have reported in a letter⁵ that the higher energy levels, having mostly a O_{2p} atomic contribution, are sufficiently modified to be observed experimentally. With these premises we have first attempted to detect possible modifications in the XPS valence spectra of various hexagonal poly(oxyethylene) samples differing in their degree of crystallinity, orientation of the crystalline zone, and lamellar or fibrillar nature. The measurements failed to reveal clear modifications owing to the morphological nature of the samples.

Poly(oxyethylene) exists in two crystalline forms, hexagonal and orthorhombic. In the hexagonal form the chain assumes a 9/5 helix with a torsional angle of 78° around the C-O bond, whereas in the orthorhombic form the chain is a 2/1 helix with a torsional angle of 63.7° . From the previously mentioned calculations this would correspond to minor changes in the valence band, but they are nevertheless worth investigating.

In this study, we report XPS measurements on hexagonal and orthorhombic poly(oxyethylene) samples, in conjunction with theoretical calculations modeling the chain structure of the samples in an attempt to identify conformational signatures in the measured valence band spectra. Before presenting and interpreting the results, it is necessary to briefly describe the methodology adopted for the theoretical part of this work.

Calculations

Model Systems. The polymer unit of the most stable form of POM, the 9/5 helix, crystallizes in the hexagonal form⁶ in the orthorhombic modification, which is stable only at room temperature and pressure, the poly(oxyethylene) chain has a 2/1 helical structure.⁷ The XPS data will be compared with model calculations on the two existing as well as on the hypothetical planar zigzag or trans-trans (tt) conformations in poly(oxyethylene). The model molecules are oligomers of increasing length, corresponding to the molecular formula $\text{CH}_3\text{O}-(\text{CH}_2\text{O})_x-\text{CH}_3$, where $x = 1, 3, 5$, or 7 . The bond lengths and bond angles used to form the model chains are reproduced in Table I; the only difference between the three structures is the value of the torsional angle, i.e., 78° , 63.7° , and 180° respectively for the hexagonal POM, orthorhombic POM,

Table I
Molecular Geometry of $\text{CH}_3\text{O}-(\text{CH}_2\text{O})_x-\text{CH}_3$ ($x = 1, 3, 5, 7$) in the "Hexagonal" Conformation⁶

bond length, Å	C-O	1.43
	C-H	1.06
bond angle, deg	C-O-C	112.3
	O-C-O	109.9
	H-C-H	109.5
torsional angle, deg	O-C-O-C	78.0

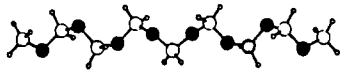
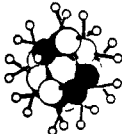
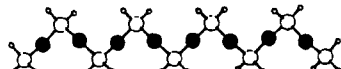
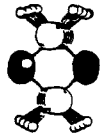

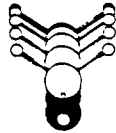
C-O-C-O DIEHEDRAL ANGLE τ ($^\circ$)	VIEW ALONG X-AXIS	TOP VIEW
78		
63.7		
180		

Figure 1. Perspective view of the $\text{CH}_3\text{O}-(\text{CH}_2\text{O})_7-\text{CH}_3$ molecules in the three studied conformations.

and planar zigzag POM. The largest molecules ($x = 7$) are represented in Figure 1.

It should be stressed that the calculations have been performed on isolated molecules, assuming that the interchain interactions affect the position and shape of all levels in the same way. This assumption seems valid in purely hydrocarbon systems such as polystyrene,³ for which Pireaux et al., from their XPS measurements, could not discriminate between amorphous and crystalline samples. In the case of highly polar macromolecules such as poly(vinyl alcohol) the polarization energy—reflecting the interchain electronic transfer during the photoelectronic process—is equal to 1.1 eV.⁸ This value for polyethylene is 0.9 eV.⁸ The behavior of this polymer, which has a degree of hydrogen bonding, is thus similar to that of van der Waals solids. However, POM is a polar compound in which the distance between the centers of the neighboring helices is about 4.5 Å. Accordingly the dipole-dipole interactions can lead to substantial broadening, as shown by Bigelow and Salaneck⁹ for organic molecules with high dipole moments. Our choice of modeling poly(oxyethylene) systems by isolated oligomeric molecules therefore reasonably assumes that the existing bulk interactions lead to a similar homogeneous broadening for all spectral bands, and in the absence of appropriate corrections we restrict our attention to the relative positions and intensities of these bands.

Calculations. The calculations reported in this work have been carried out at the ab initio level using the Gaussian 82 series of programs.¹⁰ All integrals larger than 10^{-6} were explicitly retained, and the requested convergence on the density matrix was fixed up to 10^{-5} . As shown in Figure 2 for $\text{CH}_3\text{O}-(\text{CH}_2\text{O})_x-\text{CH}_3$ where $x = 1, 3, 5$, and 7 and the torsional angle is 63.7° corresponding to the orthorhombic form, it is not until x reaches 7 that the theoretical simulations of the valence XPS spectra have their shape satisfactorily stabilized. Thus the sizes of the

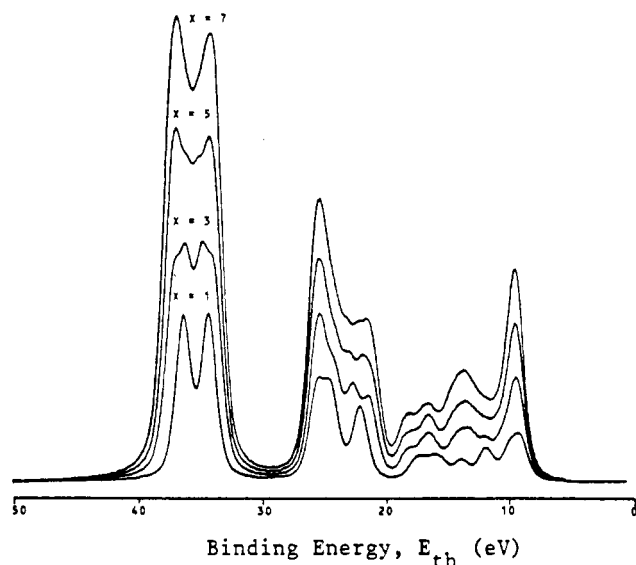


Figure 2. Theoretical simulated XPS valence band spectra of the $\text{CH}_3\text{O}-(\text{CH}_2\text{O})_x-\text{CH}_3$ molecules in the orthorhombic conformation with $x = 1, 3, 5$, and 7 .

oligomers needed to produce realistic simulations of the POM valence spectra are such that the calculations were restricted to the minimal STO-3G basis set.¹¹ The use of the more appropriate 4-31G split valence basis would correspond to 193 atomic orbitals for $\text{CH}_3\text{O}-(\text{CH}_2\text{O})_7-\text{CH}_3$, which is far too much for our present computational facilities. However, the qualitative ordering of the STO-3G energy levels was checked against previously published experimental and theoretical results on smaller but related molecular systems.^{12,13} Thus, the predicted qualitative trends in this series of compounds, which differ only by conformational modifications, are reliable.

The theoretical simulations of the valence XPS spectra for model compounds have been presented in a short Communication.⁵ They are based on the assumed validity of the frozen orbital model (Koopmans theorem) in which each line of the photoelectron spectrum is associated with an electronic orbital. The additional features originating from rotational and vibrational excitations, relaxation of the nuclear backbone, etc., which can usually be resolved in the gas-phase photoelectron spectra of small molecules, are most often hidden in the case of polymers, mainly because of the formation of band structures which may overlap and broadening effects due to the additional interactions in the solid state.

These broad bands can still be correlated with the individual molecular orbitals. By using the Gelius model¹⁴ for molecular photoionization cross sections, it is possible to obtain the shapes of the theoretical spectra in closer relationship with experiment, which facilitates the interpretation. They are constructed by the addition of peaks centered at the calculated *ab initio* energy value of the one-electron states, ϵ_k . A typical peak shape is reproduced by a linear combination of one Lorentzian and one Gaussian curve, both having the same height and width (1.5 eV) over the energy range considered. The peak height is scaled according to the intensity I_k computed from the Gelius model. Since the core atomic orbitals do not participate significantly in the valence energy region, they have been neglected. The relative atomic photoionization cross-sections used for C_{2s} , C_{2p} , O_{2s} , O_{2p} , and H_{1s} are 1.000, 0.077, 1.400, 0.159, and 0.0, respectively. However, the energy scale of the spectra thus obtained has to be contracted in order to make the comparison with experiment easier.

Table II
Total Energy Values, in ua,^a of $\text{CH}_3\text{O}-(\text{CH}_2\text{O})_x-\text{CH}_3$ Molecules in Different Conformations

C-O-C-O torsional angle, deg	x	
	3	7
180	-264.532 674	-938.968 263
63.7	-264.541 904	-939.036 871
78	-264.541 417	-939.039 610

^a 1 ua = 627.5 kcal mol⁻¹.

In spite of the approximate nature of this approach, it has been found very useful in assisting the interpretation of diverse molecular^{15,16} and polymeric systems.^{18,19} It has even been an effective tool for detecting the contamination originating from the sample support in the measured spectra of naphthalene and biphenyl systems.²⁰

Experimental Section

Samples. The morphology and crystallinity of the POM samples, prepared at the Research Institute on Polymers and Textiles, Tsukuba, Japan, have been described previously.^{6,7} Hexagonal POM has a crystallinity degree close to 100%. The needlelike single crystals are formed by molecules extended parallel to the elongation axis. The shapes of the orthorhombic crystallites are not as homogeneous (mostly scale shaped). They aggregate in spherulites with diameters of about 0.1–1 mm. Their degree of crystallinity, determined by X-ray diffraction, is also close to 100%. The two polymers are used directly in the XPS measurements without any subsequent purification or recrystallization.

XPS Measurements. The photoelectron spectra were recorded with a Hewlett-Packard 5950A spectrometer using the A1 $K\alpha$ monochromatized radiation ($h\nu = 1486.6$ eV). The sample is introduced in a vacuum chamber (pressure below 10^{-8} atm) and cooled by liquid nitrogen to 283 K. Because of the insulating properties of POM, the positive electrostatic charges left at the surface by the emitted photoelectrons are neutralized by the use of an electron flood gun. The reproducibility of the XPS valence band spectra was checked on at least two independent sets of measurements. The calibration of the spectra was performed by mixing polyethylene and referencing the spectral lines to the polyethylene C_{1s} core energy level fixed at 284.6 eV. Radiation damage at the surface of the samples during the XPS measurements was carefully checked by monitoring the shape of the C_{1s} peak before and after recording the valence band spectra. This leads to the conclusion that the diminution of the methoxy carbon, OCO, content is the same for both POM and does not exceed 10% of its original value.

Results and Discussion

Relative Stability of the Three Conformations. The computed energy values are summarized in Table II for the shortest ($x = 3$) and the longest ($x = 7$) model molecules considered in the three conformations characterized by the torsion angle τ , respectively equal to 63.7°, 78°, and 180°.

Though it is not the aim of this work to study the relative stability of the conformers, it is nonetheless useful to compare our results, which are based on the experimental geometries of the polymer (see Table I), with those pertaining to the theoretically optimized structures. As can be observed from data in Table II, the gauche-gauche (gg) conformation of the dimethoxymethane molecule ($\text{CH}_3\text{OCH}_2\text{OCH}_3$) is predicted to be more stable for the 63.7° twist in the $-\text{COCOC}-$ segment than for the other two angles, i.e., 78° and 180°. This is in line with previous *ab initio* results for the optimized geometry of dimethoxymethane. For instance, Van Alsenoy et al.,²¹ after complete geometry optimization at the 4-21G level, find a value of 62.38°, which is in good agreement with gas-phase electron diffraction measurements on dimethoxy-

methane, giving a torsional angle of 63.3° .²² These results provide support for the choice of the geometries used in the present study.

From dipole moment data,²³ the stabilization energy for the gg form of dimethoxymethane with respect to the trans-trans form (tt, $\tau = 180^\circ$) is estimated to be $3.4 \text{ kcal mol}^{-1}$. Reported ab initio quantum mechanical values range from 3.33 to $10.33 \text{ kcal mol}^{-1}$ respectively for the STO-3G²⁴ and 4-21G basis sets.²¹ In the case of $x = 3$ and by reference to total energy found here for the tt conformation, the computed stabilization energies are equal to 5.79 and $5.49 \text{ kcal mol}^{-1}$ for $\tau = 63.7^\circ$ and 78° , respectively. There is obviously a large difference between this value ($5.79 \text{ kcal mol}^{-1}$) and the one obtained by Gorenstein and Kar²⁴ ($3.33 \text{ kcal mol}^{-1}$), both computed at the STO-3G level. Such a difference can be attributed to the lack of geometry optimization in the present work. It is interesting, however, to notice that the difference in the stabilization energies between both conformations (5.79 and $5.49 \text{ kcal mol}^{-1}$) is small. Consequently this relative stability can easily be inverted in the case of the larger oligomers, $\text{CH}_3\text{O}-(\text{CH}_2\text{O})_x-\text{CH}_3$, $x = 5, 7$, etc., due to the increasing contribution of the electrostatic interactions between the polar unit cells.

Indeed, when considering the $\text{CH}_3\text{O}-(\text{CH}_2\text{O})-\text{CH}_3$ molecule, the "hexagonal" form ($\tau = 78^\circ$) is now $1.7 \text{ kcal mol}^{-1}$ more stable than the "orthorhombic" one ($\tau = 63.7^\circ$) and $44.8 \text{ kcal mol}^{-1}$ more than the tt form. These results are in agreement with previous calculations by Ohsaku and Imamura,²⁵ who by applying the CNDO/2 method on infinite and isolated model chains of POM, computed stabilization energies with respect to the tt form equal to 1.64 and $1.04 \text{ kcal mol}^{-1}$ respectively for $\tau = 78^\circ$ and 67.3° , and thus predict the infinite chain of POM with a torsional angle characteristic of the orthorhombic phase to be less stable than the conformation of the hexagonal phase. More recently, Karpfen and Beyer²⁶ have investigated the structure of the infinite poly(oxymethylene) chain by the ab initio crystal orbital method using a $7s3p/3s$ basis set. They find that the conformational state of lowest energy for the infinite isolated polymer corresponds to an intermediate value of the torsional angle, 70.8° , with a stabilization energy per $-\text{CH}_2\text{O}-$ units—with respect to the all-trans conformation—equal to $12.8 \text{ kcal mol}^{-1}$. However, it may be hazardous to conclude that the stability of poly(oxymethylene) can simply be inferred from single-chain calculations. A recent work by Aich and Hägele²⁷ using semiempirical potential functions suggests that the preference for the hexagonal form (78°) originates from a subtle balance between the intra- and interchain interactions.

XPS Valence Band Spectra. First, it is important to recall that it is not until x reaches 5 and 7 that the shape of the theoretical spectra are satisfactorily stabilized, as shown in Figure 2 for $\text{CH}_3\text{O}-(\text{CH}_2\text{O})_x-\text{CH}_3$ ($x = 1, 3, 5, 7$) and $\tau = 63.7^\circ$. Accordingly, and from now on, we will consider the simulated spectra of the three conformations of $\text{CH}_3\text{O}-(\text{CH}_2\text{O})_7-\text{OCH}_3$ as appropriate substitutes for the theoretical spectra of the infinite chains in the related conformations. The simulated valence band spectra of the three model molecules and the corresponding experimental spectra of the two existing POM modifications are shown in Figure 3.

Note that the experimental spectra, after subtraction of a proportional background, are smoothed in order to define clearly the position and intensity of the peaks.

Four regions, labeled A–D, can be distinguished. The binding energy and normalized intensity (with respect to

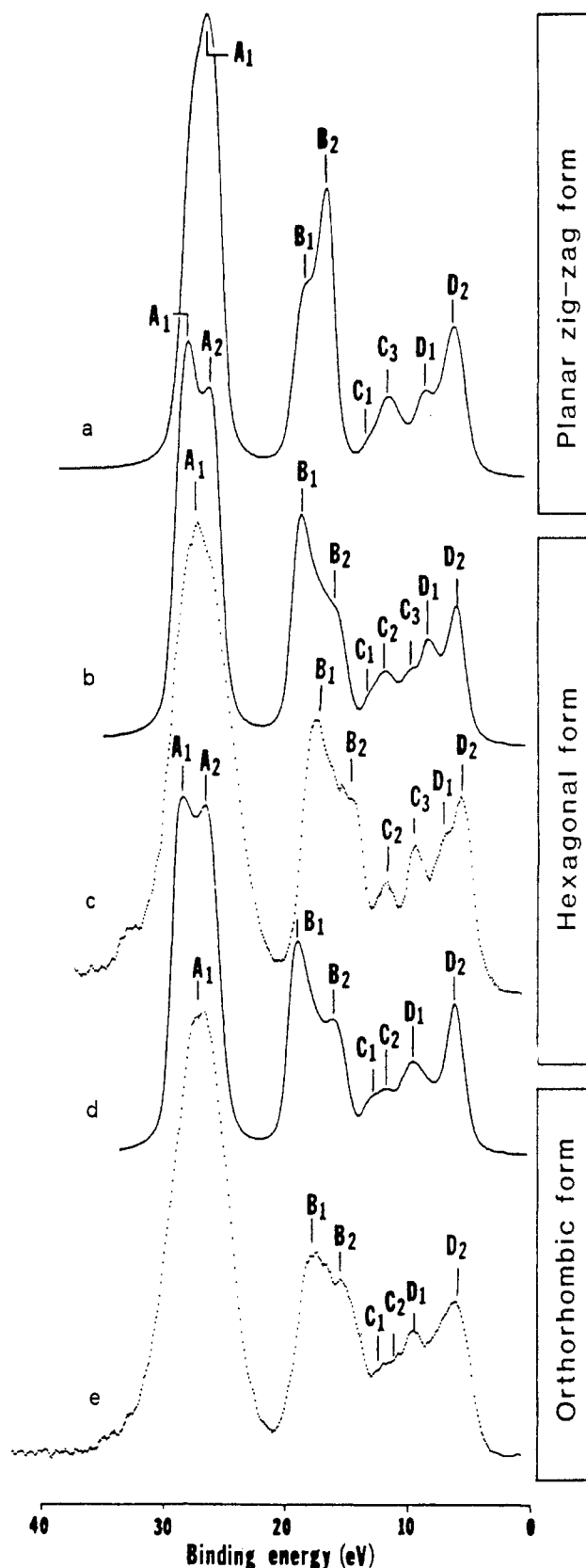


Figure 3. Theoretically simulated XPS valence band spectra of the $\text{CH}_3\text{O}-(\text{CH}_2\text{O})_7-\text{CH}_3$ molecule in the three conformations, (a) $\tau = 180^\circ$, (b) $\tau = 78^\circ$, and (d) $\tau = 63.7^\circ$, and experimental valence band spectra of hexagonal POM (c) and orthorhombic POM (e).

the O(2s) intensity peak) of their characteristic peaks are displayed in Table III. These regions respectively correspond to one electron states whose atomic orbital contributions are mainly O_{2s} , $\text{C}_{2s}-\text{O}_{2s}$, C_{2p} , and $\text{C}_{2p}-\text{O}_{2p}$. In

Table III
Position and Normalized Intensities (Printed in Heavy Type) of the Peaks Belonging to Theoretical and Experimental
Valence Band Spectra of POM ($\Delta E = 0.1$ eV)

peak label ^a	hexagonal form		orthorhombic form		trans-trans form
	theory	exptl	theory	exptl	
A ₁	36.8 (27.5) ^b 1.00	26.1 1.00	37.0 (28.3) 1.00	26.6 1.00	36.4 (27.2) 1.00
A ₂	34.3 (25.5)		34.3 (25.5)		
B ₁	25.2 (18.7) 0.59	17.6 0.56	25.4 (18.4) 0.61	17.7 0.47	25.2 (18.2) 0.41
B ₂	21.5 (15.2) 0.33	15.0 0.40	20.5 (14.4) 0.36	15.6 0.41	23.1 (16.5) 0.66
C ₁	18.4 (12.8) 0.12		18.2 (12.6) 0.15	12.4 0.22	17.4 (12.0) 0.08
C ₂	16.8 (11.5)	0.18	12.0 0.21	11.2 0.24	
C ₃	14.4 (9.6) 0.19	9.5 0.29			17.0 (11.6) 0.17
D ₁	12.3 (7.9) 0.25	7.2 0.32	13.9 (9.2) 0.24	9.6 0.29	13.2 (10.4) 0.19
D ₂	9.5 (5.6) 0.38	5.9 0.39	9.7 (5.8) 0.46	6.2 0.35	10.2 (6.2) 0.34

^a Figure 3. ^b Values in brackets are E'_{th} , obtained from E_{th} calculated values as $E'_{th} = 0.80E_{th} - 1.96$.

order to facilitate the comparison with experimental data, the theoretical energy scale is linearly contracted according to the equation

$$E'_{th} = 0.80E_{th} - 1.96$$

where E_{th} is the ab initio calculated theoretical binding energy of the peak and E'_{th} the theoretical contracted value, which will be used from now on, in comparing both experimental and theoretical spectra.

1. Comparison between Experimental and Theoretical Spectra of POM of the Same Conformation. When comparison is possible, the theoretical and experimental spectra of POM of the same conformation appear very similar both from the point of view of their overall shape and relative peak positions. In regions A and B, the theoretical simulation are in good agreement with experiment. The predicted lower intensity ratio of the B₁ peak versus the B₂ peak in the orthorhombic form, compared to the hexagonal one, is experimentally observed in spite of a noticeable difference in the peak widths. However, a shift of the B region toward higher binding energies is to be noticed (see Table III and Figure 3).

Considering the C and D regions of the "orthorhombic" isomer, the four predicted peaks are experimentally observed and their normalized intensities are satisfactorily reproduced. However, a significant difference is observed in the experimental shape of peaks C₁ and C₂ which are not so distinct as the predicted ones (Figure 3d,e). This is partly due to the overlapping of the B₂ peak (C_{2s}-O_{2s}) in the experimental spectrum. Their theoretical predicted values, E'_{th} , 12.1 and 10.8 eV are nevertheless in complete agreement with the two experimental binding energies values 12.4 and 11.2 eV, respectively.

In the case of the "hexagonal" isomer, the theoretical calculations forecast five peaks in regions C and D, while the experimental curve allows only four to be distinguished (Figure 3b,c): the experimentally missing C₁ peak is likely hidden by the broadening of the B₂ peak (C_{2s}-O_{2s}). The C₃ peak, expected at $E'_{th} = 9.6$ eV in the form of a shoulder of the D₁ peak at $E'_{th} = 7.9$ eV, appears more intense and well resolved at the same energy, 9.5 eV, in the experimental spectrum. Finally, the D₁ peak occurs experimentally at lower binding energy, 7.2 eV, than calculated and is observed as a shoulder of the D₂ peak at 5.9 eV.

2. Influence of the Conformation on the Valence Band Spectra of POM. **2.1. Regions A and B.** In all three simulated spectra, the O_{2s} peak is notably insensitive to conformational modifications, while the C_{2s}-O_{2s} or B region is more responsive to the geometry of the model molecules. Upon going from $\tau = 180^\circ$ to $\tau = 78^\circ$ and 63.7° , this region shows an inversion in the relative intensity of the B₁ (18.2 eV) and B₂ (16.5 eV) peaks. The smaller change in torsion angle τ from 78° to 63.7° , reflected in

the theoretical spectra by a larger intensity B₁/B₂ ratio in the hexagonal variety compared to the orthorhombic one, can still be traced in the experimental spectra (Table III). These features already provide evidence for conformational influences on the XPS valence band spectra of poly(oxymethylene).

2.2. Region C. Region C, mainly of C_{2p} nature, is more difficult to analyze because of the low C_{2p} photoionization cross section, resulting in a weaker signal-to-noise ratio. Nevertheless, as shown in Figure 3 and Table III, the emergence of the peak C₂ and the coming out of the peak C₃ could be observed in the theoretical as well in the experimental spectra of the "hexagonal" POM owing to the larger torsional angle of the polymeric chains. Once again the differences between the conformational varieties of POM in this region of the valence XPS spectra have a structural origin.

2.3. Region D. Before comparing and discussing the features of the D region of the XPS spectra of "orthorhombic" and "hexagonal" poly(oxymethylenes), it is useful to make a theoretical digression to provide a deeper understanding of the nature of the topmost occupied molecular orbitals and their evolution with torsional angle. To simplify the analysis we only consider the case of the simpler dimethoxymethane molecule. In the upper part of Figure 4, the skeleton of the molecule is schematically represented for the three τ values. In the lower part of the figure are given the patterns of the 2p atomic functions, as they occur in the highest occupied molecular orbital (HOMO) and the next highest occupied molecular orbital (HOMO-1). They are sorted according to the Cartesian orientations. The evolution of the one-electron levels with dominant C_{2p} and O_{2p} contributions are represented in Figure 5 with respect to chain length increase for all three conformations.

It is important to note that the O_{2p} atomic functions are the essential constituents to the HOMO and HOMO-1 levels characteristic of the D region. In the tt conformation the O_{2px} atomic orbitals in the HOMO undergo a destabilization due to "through bond" interaction, via the π -methylene group where both the C_{2px} and the H_{1s} (not represented in the figure) atomic functions contribute. In the HOMO-1, the O_{2px} atomic functions are essentially noninteracting. In the gauche forms, as can be seen from the weights of the atomic functions given in the figure, due to the torsion angle around the C-O bonds, there is a reduction in the antibonding character of the HOMO. Relative to the tt conformation, the destabilization of the HOMO-1 is seen from the weight pattern of the C_{2pz} and O_{2pz} functions. These features qualitatively explain the smaller separation in dimethoxymethane between the π -type levels indicated in Figure 5 for the gauche conformations: 0.10 and 0.23 eV respectively for $\tau = 63.7^\circ$ and

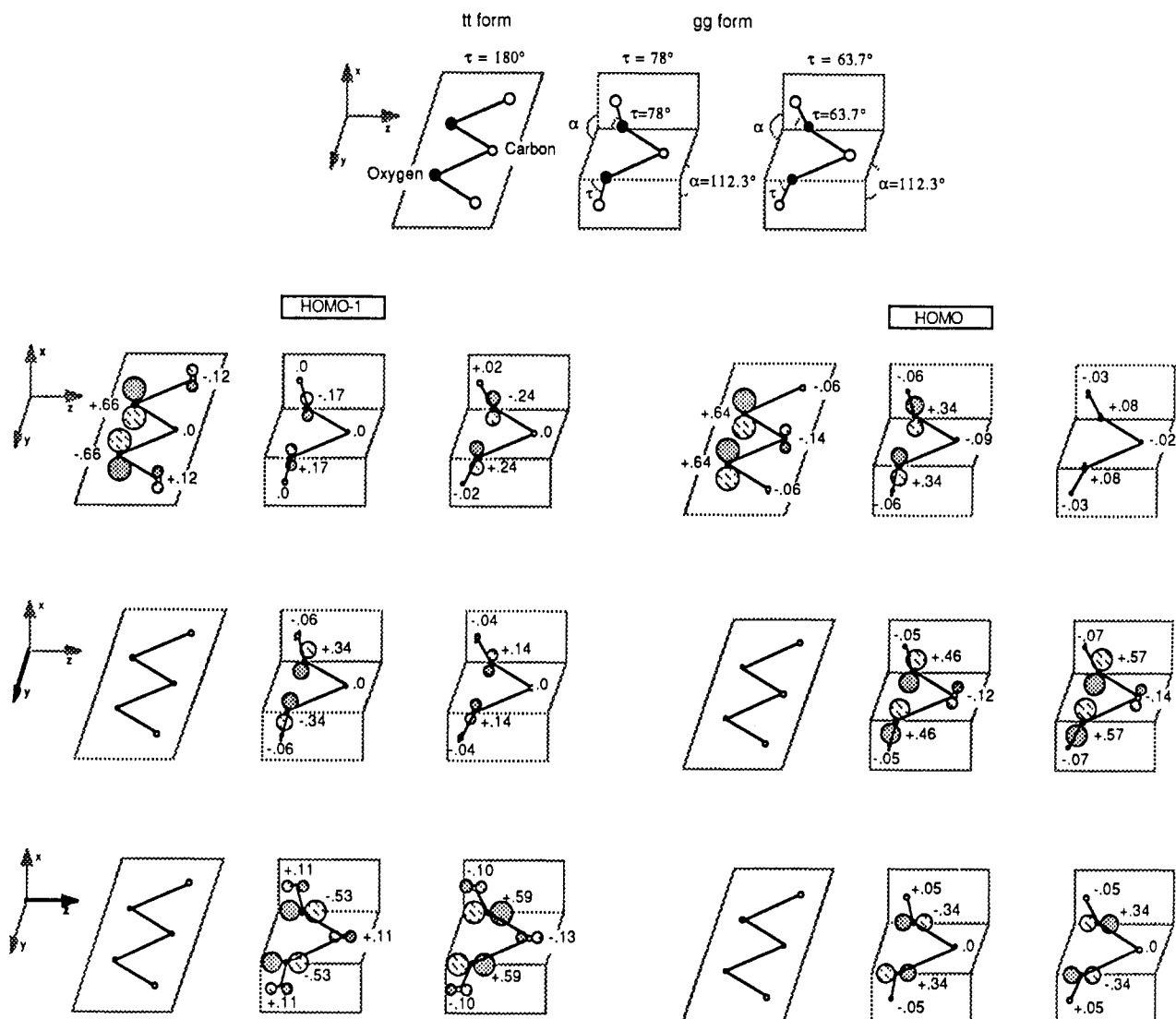


Figure 4. Patterns of highest (HOMO) and near highest (HOMO-1) occupied molecular orbitals in the dimethoxymethane molecule for the three studied conformations.

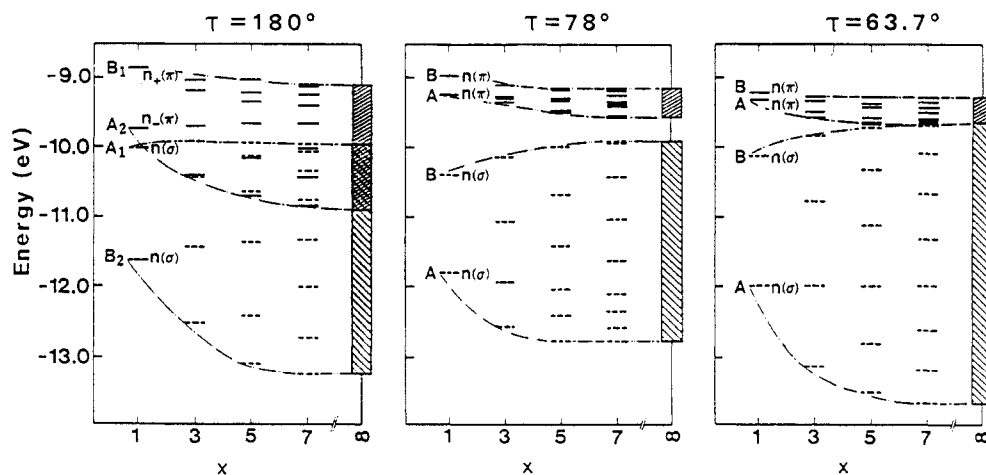


Figure 5. Influence of the torsional angle on the distribution of the topmost π (continuous line) and σ (broken line) occupied levels (mostly $O_{2p}-C_{2p}$ character) in $-(CH_2O-)_x-$ systems where $x = 1, 3, 5, 7$, and consecutively on the formation of the corresponding π and σ bands for x infinite.

78°, compared to the tt form, 0.82 eV. Our results are in qualitative agreement with the previously published theoretical results by Jörgensen et al.,^{12,13} based on nonempirical PRDDO molecular orbital calculations. For the gg form with $\tau = 66.7^\circ$ they obtain a value of 0.01 eV and for the tt form, 0.69 eV. In this study they also determined

by gas-phase UPS measurements the corresponding splitting for dimethoxymethane, 0.24 eV; for the *trans*-1,8-dioxadecaline, considered as a model molecule for the tt conformation, they measure 0.85 eV.

As expected for molecules of increasing size, the HOMO and HOMO-1 levels develop into bands of levels. This

band is particularly large in the case of the tt form and partially overlapping with the levels denoted $n(\sigma)$ in Figure 5. The corresponding band is narrower for the two gg forms, owing to the torsion angles, which reduce the "through-bond" interactions. However, in the case of $\tau = 63.7^\circ$, the bottom of the π -type band is shifted toward lower energies compared with $\tau = 78^\circ$.

This theoretical information can now be compared with experiment. Here again there is reasonable agreement between the theoretical and experimental D_1 and D_2 peaks, both in shape and energies. The most significant difference is in the obvious overestimation by theoretical calculations of the D_1 - D_2 splitting in the "hexagonal" form (see Figure 3). Compared to $\tau = 78^\circ$, the larger splitting of the $n(\sigma)$ levels (Figure 5) in the case of $\tau = 63.7^\circ$ leads to a significant shift of the D_1 peak toward higher binding energies, up to the point that it partially overlaps the top of the C region, as is indeed observed. Furthermore, as already mentioned, the bottom of the π -type bands, predicted to be located at lower energies, is experimentally verified through the position of the D_2 peak, 5.9 and 6.2 eV respectively for the "hexagonal" and "orthorhombic" forms.

Conclusions

Quantum mechanical calculations performed on simple model molecules representing long polymer chains have proven to be successful in the prediction and interpretation of the valence band spectra of the two existing forms of the poly(oxymethylene). Although the calculations have been performed with a minimal basis set, STO-3G, and the intensities of the peaks calculated with the Gelius model, the theoretical results are generally in good agreement with experiment. This combined approach is particularly appropriate for identifying conformational signatures in the valence XPS spectra of these compounds.

Obviously, this study is a first approach, and refinements are needed at both theoretical and experimental levels. From a theoretical point of view, it would be interesting to use a more rigorous method to predict photoionization spectra, binding energies, and intensities and thereby to hope, in particular, to determine the reason for overestimating the D_1 peak shift in the "hexagonal" form. Experimentally, it would be interesting to confirm the evolution of the highest occupied one electron states by means of more sensitive and yet better resolved photoelectron spectroscopies using UV and/or synchrotron radiations.

Finally, the problem is not complete, since only the two gg forms exist as polymers in nature. However, the tt form of poly(oxymethylene) could be indirectly studied through the cyclized form of polyacrolein polymer. Theoretical and experimental work on such compounds is presently in progress.

Acknowledgment. We are very grateful to Dr. M. Iguchi from the Research Institute on Polymers and Textiles, Japan, for providing the POM samples used in this study. We also acknowledge the National Fund for Scientific Research (Belgium), IBM Belgium, and the Facultés Universitaires Notre-Dame de la Paix (FUNDP) for the use of the Namur Scientific Computing Facility.

Registry No. POM, 9002-81-7; $H_3COCH_2OCH_3$, 109-87-5; $H_3CO(CH_2O)_3CH_3$, 13353-03-2; $H_3CO(CH_2O)_5CH_3$, 13352-76-6; $H_3CO(CH_2O)_7CH_3$, 13353-04-3.

References and Notes

- (1) Delhalle, J.; André, J. M.; Delhalle, S.; Pireaux, J. J.; Caudano, R.; Verbist, J. J. *J. Chem. Phys.* **1974**, *60*, 595.
- (2) Delhalle, J.; Montigny, R.; Demanet, C.; Andre, J. M. *Theor. Chim. Acta* **1979**, *50*, 343.
- (3) Pireaux, J. J.; Riga, J.; Caudano, R.; Verbist, J. J. *ACS Symp. Ser.* **1981**, No. 162, 169.
- (4) Delhalle, J.; Delhalle, S.; Riga, J. *J. Chem. Soc., Faraday Trans. 2* **1987**, *83*.
- (5) Boulanger, P.; Lazzaroni, R.; Verbist, J.; Delhalle, J. *Chem. Phys. Lett.* **1986**, *129*, 275.
- (6) Iguchi, M.; Murase, I.; Watanabe, K. *Br. Polym. J.* **1974**, *6*, 61.
- (7) Iguchi, M. *Polymer* **1983**, *24*, 915.
- (8) (a) Seki, K.; Karlson, U. O.; Engelhardt, R.; Koch, E. E.; Schmidt, W. *Chem. Phys.* **1984**, *91*, 459. (b) Xian, C. S.; Seki, K.; Inokuchi, H.; Hashimoto, S.; Ueno, N.; Sugita, K. *Bull. Chem. Soc. Jpn.* **1985**, *58*, 890.
- (9) Bigelow, R. W.; Salaneck, W. R. *Chem. Phys. Lett.* **1982**, *89*, 430.
- (10) Binkley, J. S.; Frisch, M. J.; De Frees, D. J.; Raghavachari, K.; Whiteside, R. A.; Schlegel, M. B.; Fluder, E. M.; Pople, J. A. *Gaussian 82*; Carnegie-Mellon University: Implemented for the Dec 20/60 by J. G. Fripiat.
- (11) Hehre, W. J.; Ditchfield, R.; Stewart, R. F.; Pople, J. A. *J. Chem. Phys.* **1970**, *52*, 2769.
- (12) Jørgensen, F. S.; Nørskov-Lauritsen, L. *Tetrahedron Lett.* **1982**, *23*, 5229.
- (13) Jørgensen, F. S. *J. Chem. Res. Synop.* **1981**, 212.
- (14) Gelius, U. *J. Electron Spectrosc. Relat. Phenom.* **1974**, *5*, 985.
- (15) Boutique, J. P.; Riga, J.; Verbist, J. J.; Delhalle, J.; Fripiat, J. G.; André, J. M.; Haddon, R. C.; Kaplan, M. L. *J. Am. Chem. Soc.* **1982**, *104*, 2691.
- (16) Boutique, J. P.; Riga, J.; Verbist, J. J.; Delhalle, J.; Fripiat, J. G. *J. Electron Spectrosc. Relat. Phenom.* **1984**, *33*, 243.
- (17) Boutique, J. P.; Riga, J.; Verbist, J. J.; Delhalle, J.; Fripiat, J. G.; Haddon, R. C.; Kaplan, M. L. *J. Am. Chem. Soc.* **1984**, *106*, 312.
- (18) Delhalle, J.; Delhalle, S.; André, J. M. *Chem. Phys. Lett.* **1975**, *34*, 430.
- (19) Delhalle, J.; Delhalle, S.; André, J. M.; Pireaux, J. J.; Riga, J.; Caudano, R.; Verbist, J. J. *J. Electron Spectrosc. Relat. Phenom.* **1977**, *12*, 293.
- (20) Riga, J.; Boutique, J. P.; Verbist, J. J.; Delhalle, J.; Fripiat, J. G. *J. Electron Spectrosc. Relat. Phenom.* **1984**, *33*, 312.
- (21) Van Alsenoy, C.; Schäfer, L.; Scarsdale, J. N.; William, J. O.; Geise, H. J. *J. Mol. Struct.* **1981**, *86*, 111.
- (22) Astrup, E. E. *Acta Chem Scand.* **1973**, *27*, 3271.
- (23) Uchida, T.; Kurita, Y.; Kubo, M. *J. Polym. Sci.* **1956**, *29*, 365.
- (24) Gorenstein, D. G.; Kar, D. *J. Am. Chem. Soc.* **1977**, *99*, 672.
- (25) Ohsaku, M.; Imamura, A. *Macromolecules* **1978**, *11*, 970.
- (26) Karpfen, A.; Beyer, A. *J. Comput. Chem.* **1984**, *5*, 19.
- (27) Aich, R.; Hägele, P. C. *Progr. Colloid Polym. Sci.* **1985**, *71*, 86.